

The use of a rotating cylinder electrode to selective recover palladium from acid solutions used to manufacture automotive catalytic converters

J. E. Terrazas-Rodríguez · S. Gutiérrez-Granados ·

M. A. Alatorre-Ordaz · C. Ponce de León ·

F. C. Walsh

Received: 25 January 2010/Accepted: 5 September 2010/Published online: 28 September 2010
© Springer Science+Business Media B.V. 2010

Abstract The reduction of palladium, rhodium and neodymium ions at concentrations of 0.94, 0.97 and 0.69 mol dm⁻³, respectively was studied in 1 mol dm⁻³ HNO₃ or 1 mol dm⁻³ HCl, at a stainless steel and a vitreous carbon electrode, at 25 °C. At a vitreous carbon electrode in a solution containing rhodium and palladium ions in 1 mol dm⁻³ HCl electrolyte, the reduction of metal ions occurred at a similar potential to the formation of hydrogen gas, which impeded the selective separation of the two metals. At a stainless steel cathode in 1 mol dm⁻³ HNO₃, palladium deposition occurred at a potential ≈ 0.35 V less negative than that of rhodium allowing the selective recovery of palladium. Neodymium ions were not electroactive in acidic chloride or nitrate media at pH 0. Using a solution obtained from a catalytic converter manufacturer containing palladium, rhodium and neodymium ions in 1 mol dm⁻³ HNO₃, palladium ions were preferentially removed at 0.15 V versus SHE at an average cumulative current efficiency of 57%.

Keywords Catalytic converters · Metal recovery · Neodymium · Platinum group metals · Palladium · Rhodium · Rotating cylinder electrode

1 Introduction

The active material in automotive catalytic converters is generally prepared by successive impregnations of ceramic substrates (typically zeolites) using solutions containing catalytic coating materials. The first impregnation, known as the wash coat, includes a suspension of aluminium oxide with a mixture of cerium oxides, lanthanum and neodymium ions in nitric or/and citric acid, used as a dispersant [1]. A second impregnation involves the platinum group metals (PGMs), typically as nitrate salts of Pt, Pd and Rh dissolved in nitric acid. Following these impregnations, the substrate is dried and treated at ≈ 500 °C to generate PGM oxides, which break down the partially combusted fuel [1, 2].

The impregnation processes generate dilute solutions of Pd, Rh and Nd in HNO₃ with a high concentration ratio of neodymium to palladium (2:1) and neodymium to rhodium (80:1). This high concentration of neodymium does not allow the efficient impregnation of the PGMs and the solutions need to be refurbished. This includes increasing the original PGM concentration and adjustment of the additives. The value of the catalyst contained in these solutions represents a significant asset for the industry and recovery is important to ensure a continuous supply of PGM and to avoid metal wastage. Moreover, metal recovery from waters is essential before discharge into the municipal waste water network and to avoid pollution of rivers. Possible recovery methods include cyanide treatment [3], solvent extraction [4] chemical precipitation [5, 6] photocatalytic and hydrazine reductions [7], supercritical fluids [8] and biosorption [9]. These methods suffer from poor selectivity and the high cost of chemical reagents together with sophisticated and expensive equipment. In contrast, the high selectivity, low cost and zero

J. E. Terrazas-Rodríguez · S. Gutiérrez-Granados ·

M. A. Alatorre-Ordaz (✉)

Departamento de Química, Universidad de Guanajuato,
Cerro de la Venada S/N, Pueblito de Rocha, CP 36040
Guanajuato, Gto, México

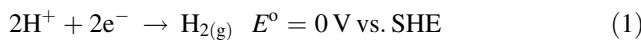
e-mail: alatorre@quijote.ugto.mx

C. Ponce de León · F. C. Walsh

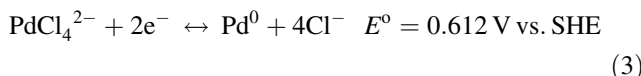
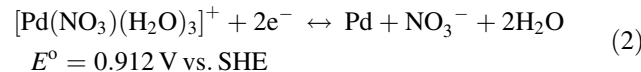
Electrochemical Engineering Laboratory, Energy Technology Research Group, School of Engineering Sciences, University of Southampton, Highfield, Southampton SO17 1BJ, UK

generation of waste chemicals in electrochemical processes render a more attractive alternative for PGM recovery. In the case of rhodium and palladium, the recovered metals can be re-dissolved in H_2SO_4 or HNO_3 to be reused. Sufficient separation between the deposition potential of each ion facilitates an effective selective recovery of the electroactive components [10, 11].

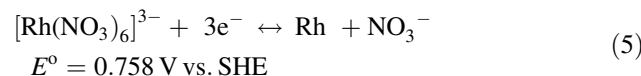
Palladium is a well established catalyst for fuel cells, hydrogenations and hydrogen adsorption processes. It can be deposited on vitreous carbon [12], gold [13], platinum [14] and silica [15]. It can also increase the corrosion resistance of stainless steel [16] but hydrogen ions can be adsorbed within the crystal lattice causing internal stresses. The latter can be avoided by using palladium complexes with reduction potentials readily separated from the hydrogen evolution reaction (HER). During the reduction of these complexes, both chemical and electrochemical reactions occur [17]. Typical ligands include CN^- and NH_3 with equilibrium constants in the order of 1×10^{51} and 1×10^{30} , respectively together with standard potentials (E°) of -0.557 and 0.034 V versus SHE, respectively [18]. These values indicate very stable complexes with reduction potentials close or negative to that of the HER:



The interaction of palladium with other ligands, such as NO_3^- or Cl^- , is not as strong as with CN^- and NH_3 and the stability constants for NO_3^- or Cl^- , are 1×10^{11} [17] and $1 \times 10^{0.17}$ [18], respectively. The reduction of these complexes occurs via the following equilibria:



The E° value of these complexes is very positive compared to the HER and suggests that palladium deposition can be readily achieved in the absence of hydrogen evolution. The reduction of rhodium ions contained in the spent impregnation solution:



might interfere during palladium recovery. The potential values for the HER and the reduction of the palladium complexes are pH dependent and the palladium deposit can be non-compact, brittle, highly stressed or powdery when accompanied by hydrogen evolution.

In this work, the electrodeposition of palladium ions from an electrolyte containing rhodium and neodymium ions in HNO_3 or HCl was studied on vitreous carbon and stainless steel electrodes. The study proposes the use of a rotating cylinder electrode reactor (RCER) to recover palladium from an industrial spent solution. The uniform mass transport and potential distribution of a RCER facilitates the recovery process at high cathodic current efficiency [11, 19, 20]. The electrolytes were a synthetic solution prepared in the laboratory and an industrial spent solution obtained from a Mexican company working on the production of catalytic converters. To our knowledge no other studies in the literature have reported the recovery of palladium from industrial effluents used for the fabrication of catalytic converters, including the figures of merit, reported work includes synthetic solutions prepared in the laboratory while normalized performance parameters are rarely considered.

2 Experimental conditions

2.1 Three-electrode electrochemical cell

A glassy carbon electrode (GCE) or AISI grade 304 stainless steel (SS304) working electrode of 0.192 and 0.07 cm^2 , respectively was used in a typical three electrode cell of 50 cm^3 working electrolyte volume. The electrodes were polished with SiC paper (600 and 1,200) followed by a felt microcloth (Buehler®) in water with decreasing grades of alumina (1.0, 0.3 and $0.05 \mu\text{m}$) rinsed with deionised water then ultrasonicated in pure water for 5 min. The counter and reference electrodes were platinum wire and Ag/AgCl (KCl sat), respectively. Measured potentials were converted to the standard hydrogen electrode (SHE) scale.

The synthetic electrolyte was prepared with $\text{Pd}(\text{NO}_3)_2$, $2\text{H}_2\text{O}$, $\text{Rh}(\text{NO}_3)_3$ (Johnson Matthey) and Nd_2O_3 (Rhodia Electronics and Catalysis) at 0.94 (100 mg dm^{-3}), 0.97 (100 mg dm^{-3}) and 0.69 (100 mg dm^{-3}) mmol dm^{-3} , respectively, in 1 mol dm^{-3} HNO_3 or 1 mol dm^{-3} HCl at 25°C . The solutions were deoxygenated with N_2 for 10 min before each experiment. A potentiostat-galvanostat (PARC 273) PC controlled with Powersuite 256 software was used. The composition of the industrial solution was $22.2 \text{ mmol dm}^{-3}$ ($2,368 \text{ mg dm}^{-3}$) Pd^{2+} , $0.47 \text{ mmol dm}^{-3}$ (46 mg dm^{-3}) Rh^{3+} and $33.1 \text{ mmol dm}^{-3}$ ($4,776 \text{ mg dm}^{-3}$) Nd^{3+} in 1 mol dm^{-3} HNO_3 . The deposits were analyzed with a scanning electron microscope coupled with an energy-dispersive spectrometer, SEM/EDS, JEOL 6390LV/LGS.

2.2 Electrolysis in the RCER

An undivided rotating cylinder electrode reactor of 420 cm^3 capacity was fitted with a 304 grade stainless steel

cathode of 3.8 cm diameter and 11 cm length (107 cm^2) surrounded by four planar graphite anodes ($14 \times 1.8 \times 1.1 \text{ cm}$) as shown in Fig. 1. The rotating cylinder electrode (RCE) was wet polished with 800 grade SiC paper and washed with distilled water before each experiment. A DC power supply (BK Precision® 1788) was used to apply a constant cell voltage of 3 V between cathode and anodes while the cathode potential, measured with a reference electrode and a high impedance digital voltmeter (DVM), was 0.15 V versus SHE. This value minimized the HER rate and ensured that palladium reduction was the main cathode reaction. An AC motor (OTMT®) with 4/5 HP and stepless variable speed was used to rotate the RCE. The rotation rate was 280 rev min^{-1} as it was found that palladium re-dissolved into the $1 \text{ mol dm}^{-3} \text{ HNO}_3$ solution at

higher rotation rates. All experiments were carried out in duplicate and the electrolysis lasted approximately 3 h. A 1 cm^3 aliquot was taken from the electrolyte every 10 min to analyse the concentrations of Pd, Rh and Nd with a plasma mass spectrometer (Agilent Technologies, 7500 inductively coupled, Tokyo, Japan) fitted with a Meinhard nebulizer, a Peltier-cooled spray chamber (-2.1°C) and an octopole collision/reaction cell with H_2 gas pressurization (purity 99.999%).

3 Results and discussion

3.1 Study of the synthetic solutions using a vitreous carbon electrode

3.1.1 Palladium deposition

Figure 2 shows the cyclic voltammogram of $0.94 \text{ mmol dm}^{-3} \text{ Pd}^{2+}$ ions in $1 \text{ mol dm}^{-3} \text{ HCl}$ and HNO_3 . In HCl electrolyte (dashed line) the current increased gradually and a sudden rise was observed at 0.05 V versus SHE with a short steep plateau between -0.05 and -0.075 V versus SHE due to the reduction of the palladium chloro-complex ions (reaction (3)) [17, 20]. The adsorption of hydrogen on the newly formed palladium particles followed by the HER, negative to -0.1 V versus SHE are the cause of the current increase after the steep plateau [21]. During the reverse potential sweep, the reduction of palladium was still observed after the crossing at 0 V versus SHE and shows that the vitreous carbon surface was modified by palladium deposition. The crossover at $\approx 0.35 \text{ V}$ versus

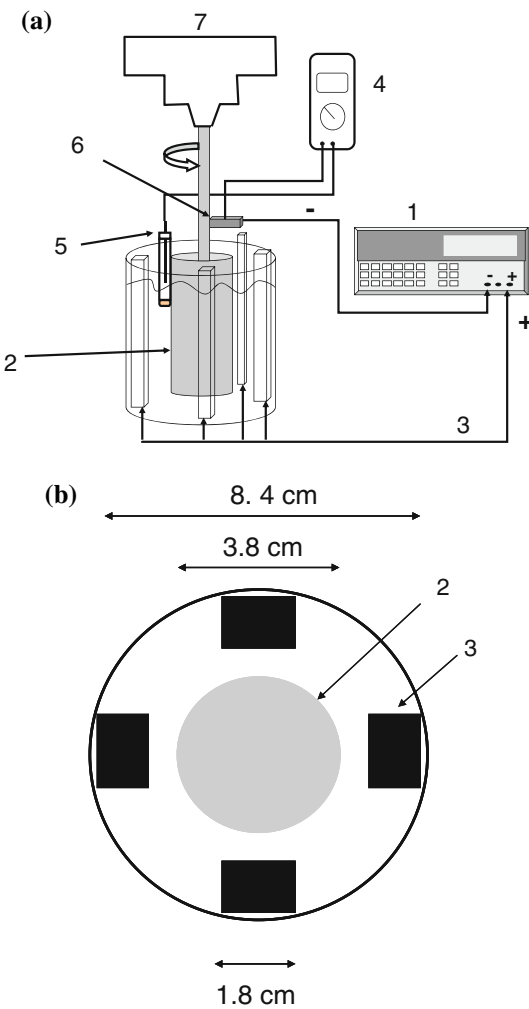


Fig. 1 The rotating cylinder electrode reactor (a) general view of the cell, electrolyte capacity, 0.42 dm^3 : 1 power supply, 2 stainless steel cathode, 107 cm^2 , 3 4 graphite anodes (each 56 cm^2), 4 digital voltmeter, 5 Ag/AgCl reference electrode, 6 electrical connector, 7 electrical motor. (b) View from the top of the rotating cylinder electrode

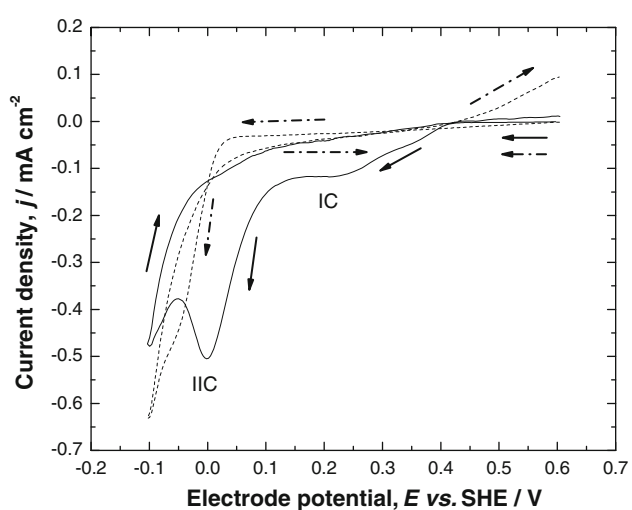


Fig. 2 Cyclic voltammograms at a vitreous carbon electrode (0.196 cm^2) in $0.94 \text{ mmol dm}^{-3} \text{ Pd}^{2+}$ in $1 \text{ mol dm}^{-3} \text{ HCl}$ (dashed line) or $1 \text{ mol dm}^{-3} \text{ HNO}_3$ (continuous line) at a linear potential sweep rate of 10 mV s^{-1} and 25°C

SHE indicates a slight oxidation of palladium on the modified surface [22]. These results show that palladium deposition overlaps with the HER suggesting that selective removal of palladium ions in HCl electrolyte with a high current efficiency might be difficult.

In the case of palladium electrodeposition from a 0.94 mmol dm⁻³ solution at a vitreous carbon cathode in 1 mol dm⁻³ HNO₃ (Fig. 2, continuous line) the current increased at 0.425 V versus SHE and a plateau (IC) could be observed between 0.08 V ≤ E versus SHE ≤ 0.2 V due to the reduction of palladium ions (reaction (2)) [17, 18]. The second process (IIC) at -0.07 V ≤ E versus SHE ≤ 0.02 V is characteristic of the electrosorption of hydrogen. After these two processes the current increased due to the HER. The clear separation between the processes IC and IIC suggests that selective separation of palladium in HNO₃ is possible.

3.1.2 Rhodium deposition

The open circuit-potential (OCP) of 0.97 mmol dm⁻³ rhodium ions in 1 mol dm⁻³ HCl is 0.6 V versus SHE in the vitreous carbon electrode but the current only increased at -0.15 V versus SHE (Fig. 3, dashed line). This is due to the reduction of rhodium ions according to reaction (4) which causes the instantaneous adsorption of protons and hydrogen gas [17, 23, 24] but the two processes cannot be distinguished. The slightly larger current during the reverse potential sweep, until the crossover at 0.05 V versus SHE, shows that rhodium is still being deposited and that the surface has been modified despite the absence of an oxidation current.

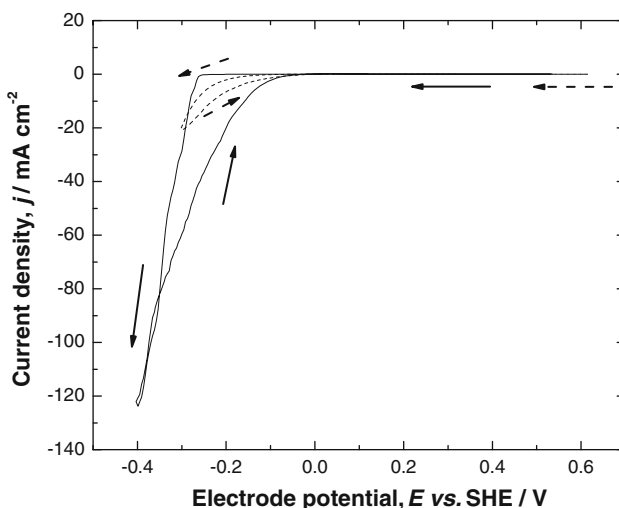


Fig. 3 Cyclic voltammograms at a vitreous carbon electrode (0.196 cm²) in 0.97 mmol dm⁻³ Rh³⁺ in 1 mol dm⁻³ HCl (dashed line) or 1 mol dm⁻³ HNO₃ (continuous line) at a linear potential sweep rate of 10 mV s⁻¹ and 25 °C

Figures 2 and 3 (dashed lines) show that the reduction of palladium and rhodium ions, in HCl occurred at 0.07 and 0.15 V versus SHE, respectively making the electrochemical separation of these metals difficult in this electrolyte. Despite this, a steep plateau for palladium reduction is seen with no reduction features for the reduction of rhodium.

The reduction of 0.97 mmol dm⁻³ rhodium ions in 1 mol dm⁻³ HNO₃ (Fig. 3, continuous line) exhibited similar characteristics to the reduction observed in HCl; large overpotential before the reduction started at -0.3 V versus SHE with a steep current reaching -120 mA cm⁻² at -0.4 V versus SHE, ca. 6 times larger than in HCl. The large current is due to several processes occurring simultaneously: reduction of the rhodium complex, [Rh(NO₃)₆]³⁻, followed by reaction (5), the reduction of nitrate to nitrite ions and hydrogen adsorption [25–27].

Figure 2 (continuous line) shows that palladium reduction in 1 mol dm⁻³ HNO₃ occurred ≈ 0.35 V earlier than rhodium in 1 mol dm⁻³ HNO₃ (continuous line Fig. 3) facilitating the selective separation of the ions in this electrolyte.

3.1.3 The presence of neodymium ions

The cyclic voltammetry of 0.69 mmol dm⁻³ of Nd³⁺ in 1 mol dm⁻³ HCl or 1 mol dm⁻³ HNO₃ showed no distinctive electrochemical processes. This is consistent with the predicted redox potential of Nd³⁺ at $E^\circ = -2.4$ V versus SHE and shows that the presence of Nd³⁺ is unlikely to affect the reduction of Pd²⁺ and Rh³⁺ ions. Neodymium is difficult to reduce as shown by the fact that can be extracted from Nd₂O₃ by electrolysis at 900 °C at vitreous carbon or tungsten electrodes [28].

3.2 Synthetic solutions and a stainless steel cathode

Stainless steel provides a low cost robust electrode material for metal recovery compared to vitreous carbon. One disadvantage is the existence of an oxidation process of this substrate before the deposition of palladium and rhodium ions in 1 mol dm⁻³ of HCl [29]. For this reason the reduction of palladium, rhodium and neodymium was studied in HNO₃ only.

3.2.1 Palladium deposition

The reduction of 0.94 mmol dm⁻³ palladium ions in 1 mol dm⁻³ HNO₃ (Fig. 4, dashed line) occurred between 0.30 and 0.17 V versus SHE (IC_{Pd} process) followed by the reduction of hydrogen ions close to 0 V versus SHE (IIC_{Pd} process) [30]. The reduction features resemble those observed on vitreous carbon electrode (Fig. 2, continuous

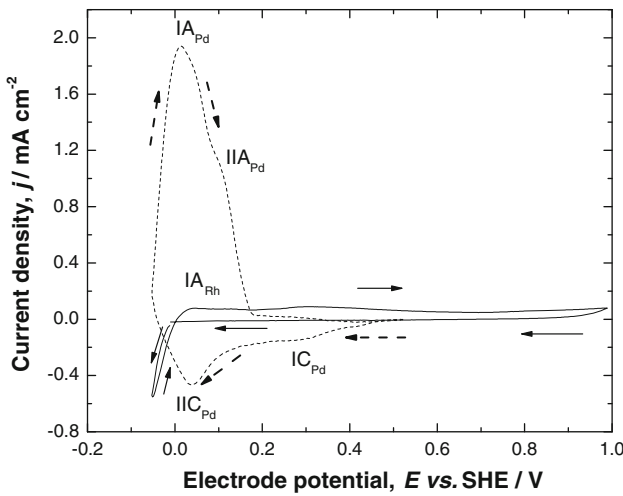


Fig. 4 Cyclic voltammograms at a stainless steel electrode in $0.94 \text{ mmol dm}^{-3} \text{ Pd}^{2+}$ ions (dashed line) in $1 \text{ mol dm}^{-3} \text{ HNO}_3$ (0.07 cm^2) at 10 mV s^{-1} and 25°C . Cyclic voltammograms at a stainless steel electrode in $0.97 \text{ mmol dm}^{-3} \text{ Rh}^{3+}$ ions (continuous line) in $1 \text{ mol dm}^{-3} \text{ HNO}_3$ at 10 mV s^{-1} and 25°C

line) except that on the SS304 electrode the hydrogen desorption process is large while in vitreous carbon is negligible. The reverse scan shows the hydrogen desorption processes, IA_{Pd} and IIA_{Pd} , at 0.02 V versus SHE and 0.10 V versus SHE, respectively [16].

3.2.2 Rhodium deposition

Figure 4 (continuous line) shows the reduction process in $0.97 \text{ mmol dm}^{-3}$ of RhNO_3 in $1 \text{ mol dm}^{-3} \text{ HNO}_3$. The OCP of this system was -0.012 V versus SHE but the current increased very rapidly as soon as the potential sweep started towards negative values. This behaviour was not observed in the background electrolyte and indicates very fast reduction of rhodium ions at the electrode surface [28]. During the reverse scan, the deposition of rhodium occurs at slightly lower potentials until the crossover at ca. 0 V versus SHE. The oxidation peak, IA_{Rh} , is associated with hydrogen desorption at rhodium.

3.2.3 The presence of neodymium ions

Neodymium ions did not show any electrochemical activity within the potential range studied on a stainless steel 304 electrode in $1 \text{ mol dm}^{-3} \text{ HNO}_3$ electrolyte [27, 28].

3.2.4 Cyclic voltammetry of Pd and Rh ions at stainless steel electrode in HNO_3 solution

A mixture of $0.94 \text{ mmol dm}^{-3}$ rhodium ions and $0.97 \text{ mmol dm}^{-3}$ palladium ions in $1 \text{ mol dm}^{-3} \text{ HNO}_3$ was used to investigate the effect of rhodium ions on palladium

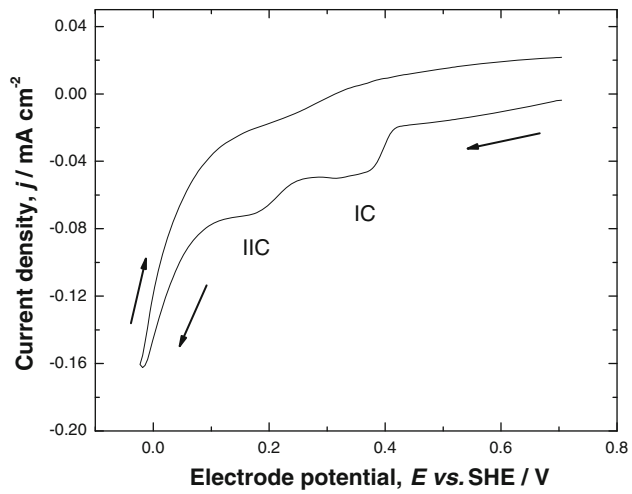


Fig. 5 Cyclic voltammograms at a stainless steel electrode (0.07 cm^2) in $0.94 \text{ mmol dm}^{-3} \text{ Pd}^{2+}$ plus $0.97 \text{ mmol dm}^{-3} \text{ Rh}^{3+}$ ions in $1 \text{ mol dm}^{-3} \text{ HNO}_3$ at a 10 mV s^{-1} and 25°C

deposition. Figure 5 shows an electrochemical process (IC) between $+0.25$ and $+0.4 \text{ V}$ versus SHE associated with the reduction of Pd^{2+} followed by a second process (IIC) between $+0.08$ and $+0.16 \text{ V}$ versus SHE associated with the adsorption of hydrogen on palladium. The sudden current increase at -0.12 V versus SHE observed in Fig. 4 (continuous line) due to Rh deposition was not observed here. The OCP value (0.71 V vs. SHE, Fig. 5) was very positive compared to Rh alone (-0.012 V vs. SHE see Fig. 4). No oxidation peaks due to hydrogen desorption were observed during the reverse sweep potential. These differences indicate that the presence of palladium appears to inhibit the simultaneous electrochemical deposition of rhodium on a stainless steel electrode or that the deposition of palladium is faster. Also, rhodium ions seems to inhibit the hydrogen desorption from palladium as observed in Fig. 3. The deposition of palladium from an aqueous effluent containing metallic and no metallic ions such as Ag(I) , UO_2^{2+} , NO^{3-} , Fe(II) and Pd^{2+} has been reported [31]. The reduction of Ag(I) and Fe(II) was favoured by the palladium deposition but caused low current efficiency of palladium recovery (40%). This behaviour was not observed in this study since metallic palladium did not favour the deposition of rhodium.

3.3 Voltammetric study of the industrial sample at stainless steel electrode

Figure 6 shows the cyclic voltammogram of an industrial sample containing palladium, rhodium and neodymium ions at 22.2 , 0.47 and $33.1 \text{ mmol dm}^{-3}$ respectively, in $1 \text{ mol dm}^{-3} \text{ HNO}_3$. Two reduction processes at 0.18 V (IC) and -0.15 V versus SHE (IIC), characteristic of the reduction of palladium and the adsorption of hydrogen can

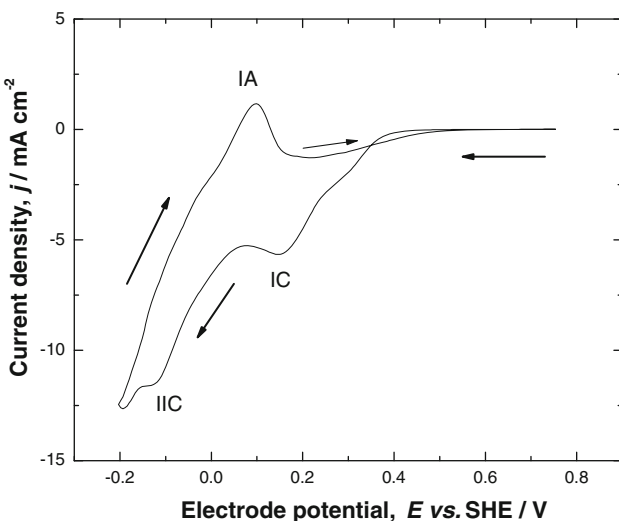


Fig. 6 Cyclic voltammogram at a stainless steel electrode (0.07 cm^2) in the industrial electrolyte containing 1 mol dm^{-3} HNO_3 at concentrations of $22.2 \text{ mmol dm}^{-3}$ Pd^{2+} , $0.47 \text{ mmol dm}^{-3}$ Rh^{3+} , $33.1 \text{ mmol dm}^{-3}$ Nd^{3+} at 10 mV s^{-1} and 25°C

be seen. These processes occur at similar potentials as those observed in Fig. 4 (dashed line) and 5 but are slightly shifted towards negative values due to the higher concentration of palladium. The hydrogen desorption processes is masked in a single broad peak (IA) in comparison with the peak and shoulder observed in the dashed line of Fig. 4.

A micro-electrolysis was carried out at the point where the peak IIC appears at 0.15 V versus SHE for 60 s . The metal deposit was observed by SEM and showed nodular features ca. $0.5 \mu\text{m}$ diameter. The powder XRD analysis showed that only palladium was deposited confirming that palladium can be selectively recovered from these industrial solutions without interference from rhodium or neodymium ions. This also shows the advantage of using HNO_3 rather than HCl as no addition of chloride would be necessary to modify the original industrial catalyst samples (which are normally stored in HNO_3).

3.4 Electrolysis in a rotating cylinder electrode reactor

Figure 7a shows the normalized concentration decay of Pd^{2+} , Rh^{3+} , and Nd^{3+} with initial concentrations of 22.2 ($2,368 \text{ mg dm}^{-3}$), 0.47 (46 mg dm^{-3}) and 33.1 ($4,776 \text{ mg dm}^{-3}$) mmol dm^{-3} , respectively, in 1 mol dm^{-3} HNO_3 during the electrolysis of the industrial solution at 0.15 V versus SHE. After 180 min , 95% of palladium and 35% of the rhodium were removed while neodymium ions remained in solution. The removal of rhodium started only until 90% of palladium was removed, after 100 min and was low: from 0.44 to $0.37 \text{ mmol dm}^{-3}$, over 180 min , suggesting that rhodium needs a palladium surface to be reduced. In fact, the electrolysis of a solution containing

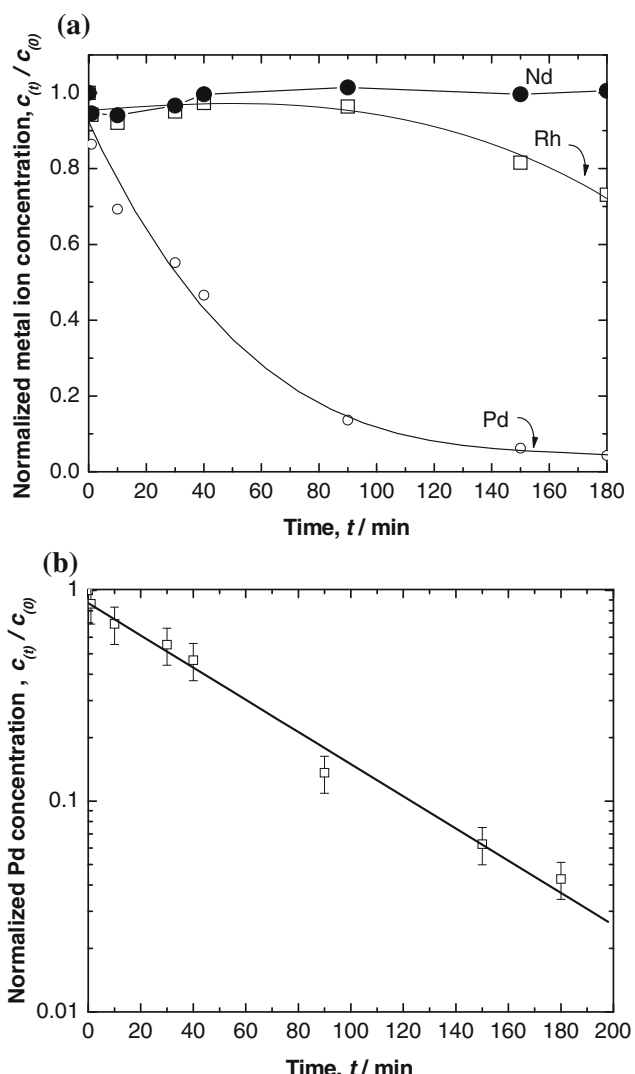


Fig. 7 (a) Normalized concentration decay of Pd^{2+} , Rh^{3+} and Nd^{3+} ions during the electrolysis at 0.15 V vs. SHE at a RCE (220 rev min^{-1}) at 25°C . The initial concentrations were 22.2 Pd^{2+} , 0.47 Rh^{3+} and $33.1 \text{ Nd}^{3+} \text{ mmol dm}^{-3}$, respectively. (b) A semi-logarithmic plot of the data in (a)

only rhodium ions in 1 mol dm^{-3} HNO_3 solution showed that no deposit occurred on a stainless steel electrode.

Assuming a first order reaction for the reduction of Pd^{2+} , the concentration decay can be expressed as [32]:

$$\log \left[\frac{c_{(0)}}{c_{(t)}} \right] = \frac{-k_m A_{\text{RCE}} t}{2.303 V_R} \quad (6)$$

where $c_{(0)}$ and $c_{(t)}$ are the palladium concentrations at the start and at time t of the batch electrolysis, respectively, k_m is the mass transport coefficient, A_{RCE} is the electrode area and V_R is the volume of the electrolyte. Figure 7b shows data from Fig. 7a treated via Eq. 6 and shows that the deposition of palladium is mass transport controlled with a calculated average mass transport coefficient k_m , of

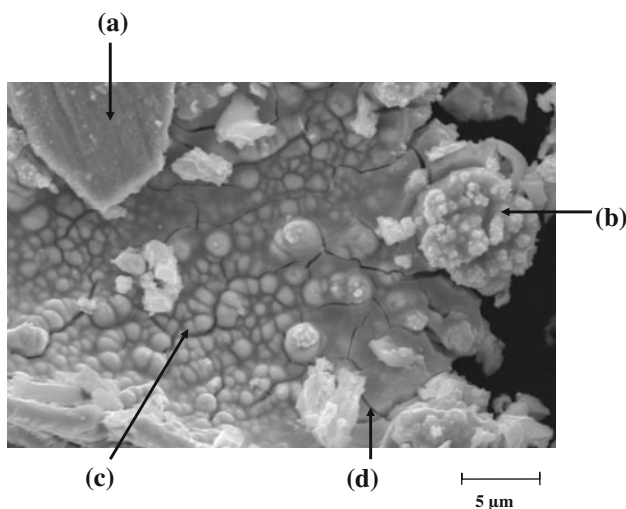


Fig. 8 SEM image of metallic palladium potentiostatically deposited at 0.15 V vs. SHE over 180 min from the industrial sample at 25 °C. Composition: 77 wt% palladium, 2 wt% copper and 1 wt% zinc and 20 wt% oxygen

1.14×10^{-3} cm s $^{-1}$. This value was used to calculate the volumetric energy consumption and specific power consumption for palladium deposition shown below.

After the electrolysis, palladium was mechanically removed from the RCE then analyzed by SEM/EDS and X-ray diffraction. The SEM image in Fig. 8 shows that palladium was deposited as broad agglomerations (a) and nodules and agglomeration of nodules of 0.5 to 1.0 μ m height (b, c), characteristic of high current densities. Similar results have been reported elsewhere [31]. The cracks (d) appeared during the mechanical removal of palladium from the RCE. Palladium was obtained as a friable black powder (black palladium) which was easily dissolved in concentrated HNO₃ and could be reused in the catalyst impregnation processes. The EDAX analysis shows that only palladium was removed from the industrial spent sample; the composition of the dry powder deposit was 77 wt% palladium, 2 wt% Cu and 1 wt% Zn, the remaining 20 wt% being oxygen. The traces of Zn and Cu were from the bronze metal used as the powder sample-holder. It is worth mentioning that some metallic rhodium could have been deposited but was not be detected with the analytical technique used (<1 wt%) and for practical applications the process can be considered selective for the extraction of palladium. These studies agree with ICP-MS analysis of the deposit which showed that palladium.

3.4.1 Figures of merit

The cumulative efficiency (ϕ), the volumetric energy consumption (E_s) [33], the normalized space velocity (s_n) [34], and the normalized volumetric power consumption

(W_n^V) for the recovery of palladium can be calculated according to the following equations [32]:

$$\% \phi = 100 \times \left(\frac{zF\Delta c_{Pd(II)} V_R}{MIt} \right) \quad (7)$$

$$E_s = \frac{zFE_{cell}\Delta c}{3.6 \times 10^3 \phi M} \quad (8)$$

$$s_n = \frac{k_m A_{RCE}}{2.303 V_R} \quad (9)$$

$$W_n^V = \frac{k_m A_{RCE} E_{cell} q}{2.303 V_n} \quad (10)$$

where z is the number of electrons, F is the Faraday constant, M is the molar mass, I is the applied current, E_{cell} is the cell voltage, Δc is the concentration difference between the time zero ($c_{(0)}$) and the time t ($c_{(t)}$) of the electrolysis, q is the overall electrical charge during the electrolysis time and V_n is the normalized volume of the electrolyte.

Figure 9 shows the current efficiency and the volumetric energy consumption versus percentage of palladium recovered during the electrolysis (Fig. 7). The current efficiency was 100% during the first 30% of palladium recovered then decreased to 57% when 95% of palladium was recovered showing a clear dependency on concentration and secondary reactions such as HER and rhodium and nitrates reduction. Despite this, the current efficiency was higher than in other works reported in the literature using synthetic solutions to simulate an effluent from the nuclear industry: in 0.1 mol dm $^{-3}$ HNO₃ (40%) [31] and in an organic solvents [35] (30%). In the present work, the palladium concentration was similar to that reported in earlier works but the electrolysis time was shorter [31]: the authors reported an 8 h electrolysis at –0.5 V versus a

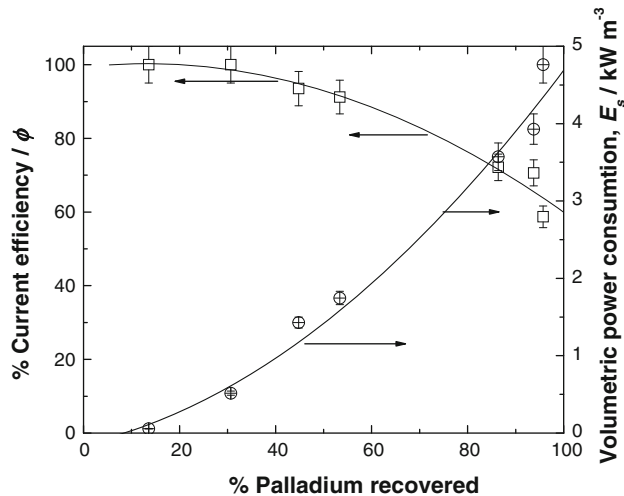


Fig. 9 Cumulative current efficiencies (left) and specific power consumption (right) for palladium removal at a RCER; data from Fig. 7

pseudo palladium reference (≈ 0.412 V vs. SHE) using a stainless steel cathode. The initial palladium concentration was 0.6 g dm^{-3} (5.6 mmol dm^{-3}) while the overall current efficiency was 30%.

The volumetric energy consumption for palladium recovery was 5 kW h m^{-3} , which is broadly similar to other industrial processes such as copper recovery ($4\text{--}7\text{ kW h m}^{-3}$) [36], tin recovery ($2\text{--}10\text{ kW h m}^{-3}$) [10], cadmium ($1\text{--}2.5\text{ kW h m}^{-3}$) [37] and cadmium recovery mixed with copper and zinc on 3-dimensional cathodes ($2\text{--}7\text{ kW h m}^{-3}$) [38]. The normalized volumetric power consumption W_n^V , was low at 1.4 kW m^{-3} showing that the electrolytic recovery method could prove affordable and selective. In addition, considering the high value of palladium (453 USD/OZ, data on 21/07/10) the low cost of the electrolysis represents a simple, viable, economic and fast option to recover platinum group metals.

The normalized space velocity, s_n , i.e. the volume of electrolyte which could be treated in a unit volume reactor with a ten-fold reduction in metal ion concentration, was $1.35 \times 10^{-4}\text{ dm}^3\text{ dm}^{-3}\text{ s}^{-1}$ which is the same order of magnitude of values reported for the recovery of 100 mg dm^{-3} of silver using a titanium RCE at 100 rpm, from solutions simulating concentrated minerals ($10 \times 10^{-4}\text{ s}^{-1}$ [39]). Also values of $0.5\text{--}3.3 \times 10^{-4}\text{ s}^{-1}$ were reported for the recovery of 500 mg dm^{-3} of cadmium on a stainless steel 316 RCE at 500 rpm at electrolysis between 0.8 and 1.4 V versus SCE [39]. In the present work, the mass of palladium removed during the 3 h electrolysis was 2,267 mg which is considerably larger than the amount removed in the previous work [34, 36] and shows the great flexibility of the RCER to deal with such effluents in a short period of time.

4 Conclusions

An electrochemical method including a rotating cylinder cathode has been used to recover palladium from spent impregnation solutions used to prepare catalytic converters. Selective palladium separation from an industrial spent solution in a rotating cylinder stainless steel electrode reactor was achieved at 57% current efficiency and specific power consumption of 4 kW h m^{-3} during the removal of 22.2 mmol dm^{-3} ($2,368\text{ mg dm}^{-3}$) of palladium. The process shows that the industrial effluent does not require addition of other acids or additives which reduces the cost and makes the process efficient and with no chemical waste.

Acknowledgments J.E. Terrazas-Rodríguez is grateful to CONACYT for his PhD scholarship, 181828. The authors are grateful to K. Wróbel, L.A. García and O. Fermín for ICP-MS, SEM analysis and contribution to the experimental work, respectively. D. Rojas provided the industrial samples via the project FOMIX GTO-2007-C02-69453, CONACYT-Guanajuato.

References

- Vigner S, Deprelle P, Hermia J (1996) Catal Today 27:229
- Wyatt M, Leach GM, Gould AS (1985) US Patent 4,500,650, 19 Feb 1985
- Chen J, Huang K (2006) Hydrometallurgy 82:164
- Hubicki Z, Leszczynska M, Lodyga B, Lodyga A (2006) Miner Eng 19:1341
- Angelidis TN (2001) Top Catal 16/17:419
- Barakat MA, Mahmoud MHH, Mahrous YS (2006) Appl Catal A Gen 301:182
- Troupis A, Hiskia A, Papaconstantinou E (2004) Appl Catal B Environ 52:41
- Iwao S, El-Fatah SA, Furukawa K, Seki T, Sasaki M, Goto M (2007) J Supercrit Fluid 42:200
- Mack C, Wilhelm B, Duncan JR, Burgess JE (2007) Biotechnol Adv 25:264
- García-Gabaldón M, Pérez-Herranz V, García-Antón J, Guiñón JL (2005) Sep Purif Technol 45:143
- Walsh FC, Gabe DR (1981) J Chem Technol Biotechnol 12:25
- Alvarez AE, Salinas DR (2005) In: Proceedings of the 2nd Mercosur Congress on Chemical Engineering and 4th Mercosur Congress on Process Systems Engineering. Rio de Janeiro, Brasil, pp 1–10
- Pandelov S, Stimming U (2007) Electrochim Acta 52:5548
- Llorca MJ, Feliu JM, Aldaz A, Clavilier J (1993) J Electroanal Chem 351:299
- Santinacci L, Djennizian T, Hildebrand H, Ecoffey S, Mokdad H, Campanella T, Schmuki P (2003) Electrochim Acta 48:3123
- Zuo Y, Tang J, Fan C, Tang Y, Xiong J (2008) Thin Solid Films 516:7565
- Rao CRK, Trivedi DC (2005) Coord Chem Rev 249:613
- Camacho Frias E, Pitsch HK, Ly J, Poitrenaud C (1995) Talanta 42:1675–1683
- Low CTJ, Ponce de León C, Walsh FC (2005) Aust J Chem 58:246
- Walsh FC (1992) In: Genders JD, Weinberg NL (eds) Electrochemical technology for a cleaner environment, Chapter 5. The Electrosynthesis Company Inc., Lancaster, NY
- Gimeno Y, Hernández Creus A, Carro P, González S, Salvarezza RC, Arvia AJ (2002) J Phys Chem B 106:4232
- Lubert KH, Guttmann M, Beyer L, Kalcher K (2001) Electrochim Commun 3:102
- Benguerel E, Demopoulos GP, Harris GB (1996) Hydrometallurgy 40:135
- Brylev O, Sarrazin M, Bélanger D, Roué L (2006) Appl Catal B Environ 64:243
- Varentsov VK, Varentsova VI (2003) Russ J Electrochem 39:703
- Belyaev AV, Fedotov MA, Khranenko SP, Emel'yanov VA (2001) Russ J Coord Chem 27:855
- Smith RM, Martell AR (1976) Critical stability constants. Plenum, New York
- Stefanidaki E, Hasiotis C, Kontoyannis C (2001) Electrochim Acta 46:2665
- Pletcher D, Urbina RI (1997) J Electroanal Chem 421:137
- Jaksic MM, Johansen B, Tunold R (1993) Int J Hydrog Energy 18:111
- Jayakumar M, Venkatesan KA, Srinivasan TG, Vasudeva Rao PR (2009) Electrochim Acta 54:1083
- Walsh FC (1995) A first course in electrochemical engineering. The Electrochemical Consultancy, Romsey, UK
- Walsh FC (1992) Bull Electrochem 8:471
- Walsh FC (1992) Electrochim Acta 38:465
- Jayakumar M, Venkatesan KA, Srinivasan TG, Vasudeva Rao PR (2009) J Appl Electrochem 39:1955

36. Rivera FF, González I, Nava JL (2008) Environ Technol 29:817
37. Grau JM, Bisang JM (2001) J Chem Technol Biotechnol 76:161
38. Walsh FC (2001) Pure Appl Chem 73:1819
39. Alonso AR, Lapidus GT, González I (2008) Hydrometallurgy 92:115